

1 **A Clinically Feasible Diagnostic Spectro-Histology Built on SERS-Nanotags for**
2 **Multiplex Detection and Grading of Breast Cancer Biomarkers**

3
4 *Vishnu Priya Murali[#], Varsha Karunakaran[#], Madhukrishnan M, Asha Lekshmi, Shamna*
5 *Kottarathil, Deepika S, Valliamma N. Saritha, Adukkadan N. Ramya, Kozhiparambil G. Raghu,*
6 *Kunjuraman Sujathan* and Kaustabh Kumar Maiti**

7
8 V.P. Murali, V. Karunakaran, Madhukrishnan M, S. Kottarathil, Deepika S, A. N. Ramya, K.K.
9 Maiti *

10 CSIR-National Institute for Interdisciplinary Science & Technology (NIIST), Chemical
11 Sciences & Technology Division (CSTD), Organic Chemistry Section, Industrial Estate,
12 Thiruvananthapuram 695019, Kerala, India.

13 K.G. Raghu

14 CSIR-National Institute for Interdisciplinary Science & Technology (NIIST), Agro-Processing
15 and Technology Division (APTD), Industrial Estate, Thiruvananthapuram 695019, Kerala,
16 India.

17 V. Karunakaran, Madhukrishnan M, A. N. Ramya, K.G. Raghu, K.K. Maiti *

18 Academy of Scientific and Innovative Research (AcSIR), Ghaziabad, 201002, India

19 A. Lekshmi, V. N. Saritha, K. Sujathan

20 Regional Cancer Centre (RCC), Division of Cancer Research, Thiruvananthapuram 695011,
21 Kerala, India

22
23 **E-mail:** kkmaiti@niist.res.in (K.K.M.)

24
25 # Both the authors contributed equally to this work

26 **Keywords:** Breast Cancer; biomarkers; SERS nanotags; multiplex detection; HER2 grading;
27 Immunohistochemistry

28 **ABSTRACT**

29 Simultaneous detection of multiple biomarkers is always an obstacle in immunohistochemical
30 (IHC) analysis. Herein, a straightforward spectroscopy-driven histopathologic approach has
31 emerged as a paradigm of Raman-label (RL) nanoparticle probes for multiplex recognition of
32 pertinent biomarkers in heterogeneous breast cancer. The nanoprobe is constructed by
33 sequential incorporation of signature RL and target specific antibodies on gold nanoparticles,

34 which are coined as Raman-Label surface enhanced Raman scattering (RL-SERS)-nanotags to
35 evaluate simultaneous recognition of clinically relevant breast cancer biomarkers i.e., estrogen
36 receptor (ER), progesterone receptor (PR) and human epidermal growth factor receptor2
37 (HER2). As a foot-step assessment, breast cancer cell lines having varied expression levels of
38 the triple biomarkers are investigated. Subsequently, the optimized detection strategy using RL-
39 SERS-nanotags is subjected to clinically confirmed, retrospective formalin-fixed paraffin
40 embedded (FFPE) breast cancer tissue samples to fish out the quick response of singleplex,
41 duplex as well as triplex biomarkers in a single tissue specimen by adopting a ratiometric
42 signature RL-SERS analysis which enabled to minimize the false negative and positive results.
43 Significantly, sensitivity and specificity of 95% and 92% for singleplex, 88% and 85% for
44 duplex, and 75% and 67% for triplex biomarker has been achieved by assessing specific Raman
45 fingerprints of the respective SERS-tags. Furthermore, a semi-quantitative evaluation of HER2
46 grading between 4+ / 2+ / 1+ tissue samples was also achieved by the Raman intensity profiling
47 of the SERS-tag, which is fully in agreement with the expensive fluorescent in situ
48 hybridization analysis. Additionally, the practical diagnostic applicability of RL-SERS-tags has
49 been achieved by large area SERS imaging of areas covering 0.5 to 5 mm² within 45 min.
50 These findings unveil an accurate, inexpensive and multiplex diagnostic modality envisaging
51 large-scale multi-centric clinical validation.

52

53 **1. Introduction**

54 Clinical biomarkers partake an imperative role in breast cancer prognosis and its heterogenous
55 as well as differential expression pattern exhibit the key challenge in choosing the proper
56 treatment modality. Hence, breast cancer biomarker detection prevails the decisive feature
57 which needs a distinct troubleshooting approach (Shah et al., 2014). The three vital prognostic
58 markers widely assessed in breast cancer diagnosis includes hormonal nuclear receptors
59 estrogen (ER) (Russo and Russo, 2006), progesterone (Lange, Carol A, 2008) and cell surface
60 human epidermal growth factor type 2/neu (HER2/neu) receptors (Costa and Czerniecki, 2020).
61 Based on these biomarker expression profiles, four major classification of breast cancer are
62 designated, viz., luminal A, luminal B, HER2 enriched and basal like subtypes (Parise and
63 Caggiano, 2014). The occurrence and extend of cell surface biomarker HER2 is often measured

64 by a grading system having 4⁺, 3⁺, 2⁺, 1⁺ and 0 grades correlating the staining intensity.
65 According to HER2 testing guidelines and samples with a staining score of 2⁺ or less is
66 considered as negative (Cornejo et al., 2014). The gold standard method immunohistochemistry
67 (IHC), which is generally employed for the detection of these biomarkers is relatively
68 inexpensive, but the results are often subjective as influenced by inter-observer variability.
69 Besides, evaluation of multiple biomarkers simultaneously in a single tissue specimen is not
70 possible, which turned out as a lengthy process to complete the investigation of all three-
71 biomarker status (Dixon et al., 2015). In the case of HER2 detection, 95 % concordance is
72 mandatory within IHC and Fluorescent in situ hybridization (FISH). FISH is a cytogenic
73 analysis to detect the number of HER2 gene copies per nucleus. Even though FISH is a robust
74 technique for HER2 detection, it necessitates expensive reagents along with laboratory
75 equipment setup (Bogdanovska-Todorovska et al., 2018; Furrer et al., 2015; Wesoła and Jeleń,
76 2015). Eventhough, techniques like multiplex immunohistochemistry/immunofluorescence
77 (mIHC/mIF) have been introduced as improved methods to detect multiple biomarkers in single
78 tissue section, its applicability has been rescricted due to several disadvantages like, limited
79 dynamic range for intensity of the chromogenic substrates in mIHC. On the other hand, mIF
80 has a large linear dynamic range for many fluorophores for quantitative analysis, however, they
81 must be chosen carefully for preventing bleed through. The highly sensitive tyramide signal
82 amplification (TSA) method is also insubstantial due to the complicated steps involved,
83 tyranide overaction and its time consuming nature (Hernandez et al., 2021; Sheng et al., 2023;
84 Tan et al., 2020). Exploration and validation of alternative simple and relatively rapid
85 techniques are always recommended which can meet acceptable diagnostic quality.

86

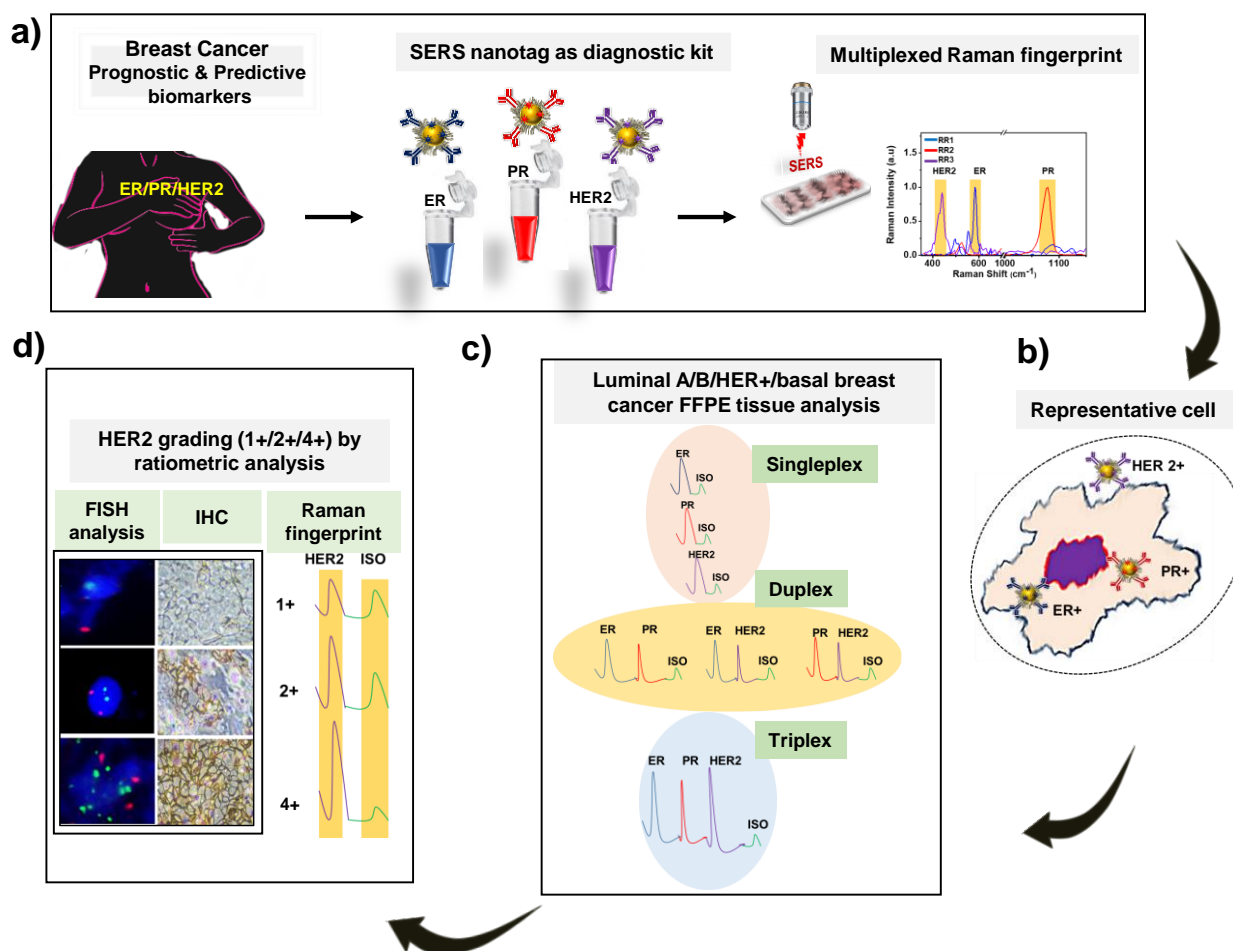
87 Surface enhanced Raman spectroscopy (SERS), is an advanced and ultrasensitive technique
88 which received immense scientific attention especially in diverse clinical diagnostic
89 applications including cancer in last several years (Haka et al., 2005; Ramya et al., 2021)

90 (Joseph et al., 2018). In diagnostic scenario, label-free SERS and Raman label -based SERS-
91 nanotags are the two major practices adopted as a detection modality so far. SERS-nanotags or
92 SERS-nanoprobes are prepared by incorporating Raman reporter molecules enabling inherently
93 strong Raman cross-section to plasmon resonant metallic nanoparticles like gold or silver.
94 Subsequently, a protective polymeric layer and a target specific recognition motif like a peptide,
95 antibody or aptamer are functionalized to the SERS-nanotags which exclusively recognize
96 specific biomarkers *in vitro*, *in vivo* and *ex vivo* specimens having moderately high
97 heterogeneity (Wang et al., 2013).

98
99 Sensitive singleplex/multiplex detection of clinically relevant cancer biomarkers utilizing
100 SERS-nanotags has shown a very promising alternative strategy, stepping up towards the
101 upcoming technology for clinical diagnostics (Dinish et al., 2014; Nariman et al., 2017; Sun et
102 al., 2021). Hence, SERS-nanotags resemble an ideal SERS-based immunoassay component for
103 the precise detection of multiplex biomarkers in a personalized manner with high sensitivity
104 and specificity (Schlücker et al., 2011).

105 Even though a few SERS-based multiplexed studies have been demonstrated for other cancer
106 types (Davis et al., 2018; Lin et al., 2021; Maiti et al., 2012; Narayanan et al., 2015; Zavaleta
107 et al., 2013) as well as breast cancer biomarkers in cells (Lee et al., 2014), serum (Li et al.,
108 2015) and fresh tissue (Wang et al., 2017) etc., there is no report so far on multiplex detection
109 of three prevalent prognostic markers *i.e.*, ER, PR and HER2 in a single tissue sample as a
110 complementary system to IHC as well as FISH analysis. Similarly, biomarker detection in fresh
111 tissue samples via topical application of SERS-tags followed by raster scanning to determine
112 surgical margin during lumpectomy has also been investigated (Y. Wang et al., 2016; Y. W.
113 Wang et al., 2016), whereas the present study prevails its distinct feature of biomarker detection
114 in the retrospective formalin fixed paraffin embedded breast tissue specimens as a parallel

115 platform that envisages to nullify the highly time consuming and subjective nature of
 116 immunohistochemistry and expensive FISH technique.



117
 118
 119 **Scheme 1.** Schematic illustration of the experimental design for differentiating the clinically relevant
 120 triple biomarkers, ER, PR and HER2. a) strategy for the multiplexed detection using ER, PR and HER2
 121 conjugated SERS-tags having AuNPs as substrate, b) representative design for detection of biomarkers
 122 in cells/paraffin embedded breast tissue samples using SERS mapping, c) Three phases of biomarker
 123 detection executed as single, dual and triple biomarker analysis from the breast tissue specimens, d)
 124 HER2 grading of IHC and FISH confirmed 1⁺, 2⁺ and 4⁺ tissue sample through ratiometric SERS
 125 mapping.

126
 127
 128 Herein, we have evaluated the clinical implementation of the multiplexing capability of the
 129 SERS technique using multiplex Raman-label SERS(RL-SERS)-nanotags to determine the
 130 breast cancer prognostic biomarkers, ER/PR/HER2 complementary to IHC. The preeminence
 131 of the study over the so far reported SERS multiplexing studies includes the clinical relevance
 132 of the selection of biomarkers and its detection in FFPE specimens, time efficient approach to
 133 analyze the maximum area of tissue samples by ratiometric large area scanning and the analysis

134 of an ambient number of different tissue subtypes in terms of biomarker status. Moreover, this
135 is the first-ever report on the semi-quantitative evaluation of HER2 grading between 4+ / 2+ /
136 1+ tissue samples by ratiometric SERS intensity profiling, in concordance with FISH analysis
137 (Scheme 1). Collectively, to establish the utility of SERS-nanotags as a next-generation clinical
138 diagnostic modality enabling a fast, facile, accurate, and reliable spectro-histologic technique
139 for multiplex prognostic analysis of heterogenous breast cancer biomarkers.

140 **2. Results and Discussion**

141 **2.1. SERS-nanotags (SERS-nanotags) for multiplex detection:**

142 Gold nanoparticles (AuNPs: 40-45 nm) were selected as a SERS substrate for the preparation
143 of SERS-nanotags to perform the multiplexing recognition of ER, PR and HER2 in breast
144 cancer due to its excellent SERS enhancement reported so far (Njoki et al., 2007). The
145 synthesized SERS substrate was characterized by UV-vis Spectroscopy, Dynamic Light
146 Scattering (DLS) and High-Resolution Transmission Electron Microscopy (HR-TEM) analysis
147 (**Figure S1a, b and c**). Further, SERS-nanotags were fabricated by tagging Raman labels
148 (reporters) having multiplexed Raman peaks which were designated *w.r.t.*, each breast cancer
149 biomarker by the respective Raman signature peak of the reporter molecule. Among three
150 Raman reporters, commercially purchased crystal violet (CV) and 4-mercapto benzoic acid
151 (MBA) were chosen based on multiplex Raman peaks at 440 and 1084 cm^{-1} respectively, along
152 with the in-house synthesized Raman reporter, squaraine di-lipoic acid (SDL) (Ramya et al.,
153 2015) with a non-overlap Raman peak at 580 cm^{-1} *w.r.t* CV and MBA.

154 The structure and the SERS fingerprint pattern of the three SERS nanotags were portrayed in
155 **Figure S2a, b, c and d**. Isotype antibody conjugated SERS-tags were prepared independently
156 with Dithio nitrobenzoic acid (DTNB) as well as 3,3 -Diethylthiacarbocyanine iodide (DTTC)
157 having signature Raman peak at 1320 cm^{-1} and 505 cm^{-1} respectively (**Figure S2e & f**). The
158 stability and biocompatibility of nanotags were improved by a protective layer of polyethylene
159 glycol (PEG) and the carboxy functionalized PEG which facilitated the conjugation of target-

160 specific antibodies. UV-Vis spectroscopy, TEM and DLS analysis of the PEGylated
161 nanoparticles were also accomplished to confirm the PEG layer formation (**Figure S1d, e and**
162 **f**). The stickiness nature and aggregation tendency of nanoparticles were minimized with the
163 employment of Tween 20 (Lin et al., 2010). The biocompatibility of the fabricated RL-SERS-
164 tags was further confirmed by cell viability assay in different breast cancer cell lines (**Figure**
165 **S3 a, b and c**). The simultaneous detection of breast cancer biomarkers was executed by
166 constructing three multiplexing RL-SERS-nanotags conjugated with the specific monoclonal
167 antibodies for the detection of clinically valid biomarkers i.e., ER, PR and HER2. The
168 successful conjugation of antibodies to AuNPs was confirmed by UV-Vis absorbance (**Figure**
169 **S4 a,b,c**) which showed a protein absorption peak around 280 nm without much compromise
170 in the SERS activity (**Figure S4 d,e,f**). Besides, polyacrylamide gel electrophoresis (PAGE)
171 analysis (**Figure S5a,b,c**) and 3, 3', 5, 5' Tetramethylbenzidine (TMB) assay (**Figure S5 d**)
172 also confirmed the presence of the tethered antibodies on the SERS-nanotags. The stability of
173 the SERS-nanotags was also monitored up to six months which ensured the stability of the
174 nanotags based on consistent SERS intensity of the signature peaks. (**Figure S6**).

175

176 *2.2. Multiplex detection by SERS-Nanotags in ER, PR and HER2 overexpressed Breast* 177 *cancer cells (Phase I):*

178 As a proof-of-principle of multiplex detection, the RL-SERS-nanotags have endeavoured in
179 breast cancer cell lines. To accomplish this, immunophenotyping was performed to ensure the
180 ER and PR abundance in MCF-7 cells as well as HER2 over-expression in SK-BR-3 cells and
181 compared with the triple negative MDA-MB-231 cells (**Figure S7a, b and c**). Further,
182 incubation time of SERS-nanotag was optimized within 2 hours (**Figure S8**). SERS analysis
183 of MCF-7 (luminal A subtype, ER⁺/PR⁺), after incubating with AuNP@SDL@anti-ER,
184 AuNP@MBA@anti-PR and AuNP@CV@anti-HER2 SERS-nanotags identified the

185 protuberant Raman signature peaks of the Raman labels SDL at 580 and MBA at 1084 cm^{-1}
186 from the nuclear location without any prominent CV peak at 440 cm^{-1} from the whole cell
187 demonstrating the effective recognition of ER and PR (**Figure S9 a-d**). Similarly, upon
188 incubation of all three nanotags with HER2-enriched breast cancer subtype SK-BR-3, resulted
189 the presence of noticeable Raman peak of CV (crystal violet) at 440 cm^{-1} from the cell surface
190 milieu (**Figure S10 a-d**). Similarly, a basal subtype($\text{ER}^+/\text{PR}^+/\text{HER2}^+$ triple negative receptors)
191 MDA-MB-231 cell line resembled a negligible expression as indicated from all the three RL-
192 SERS-nanotags ensuring the specificity of the nanotags (**Figure S11a,b and c**). A parallel
193 confirmation has been carried out for the recognition of biomarkers through RL-SERS-
194 nanotags, by dark field microscopic analysis based on the back scattering property of the
195 metallic nanoparticle uptake as detailed in the supporting information (**Figure S12 a, b and c**).

196

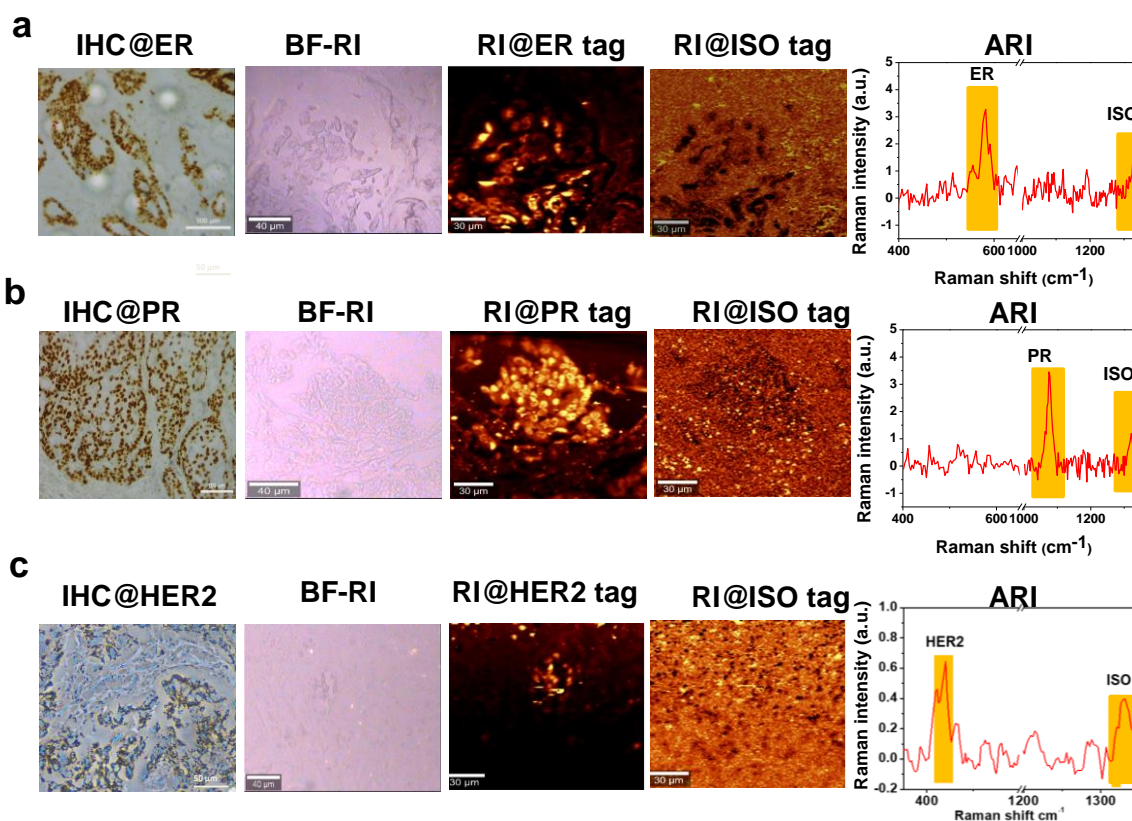
197 ***2.3. Multiplex Detection Strategy in Clinically Confirmed Breast tissue samples***

198 After the proof-of-concept confirmation in breast cancer cell lines, analysis in retrospective
199 clinical FFPE tissue sections accumulated from lumpectomy/mastectomy-derived specimens
200 was performed for the SERS detection of ER, PR, and HER2 biomarkers. Ratiometric SERS
201 evaluation was executed to detect the presence of single and multiple biomarkers, with non-
202 targeted IgG isotype antibody conjugated SERS-tags along with the targeted ones as a control
203 to minimize the false positive signal arising due to the non-specific binding. For attaining these
204 goals, three sets of detection modes were executed viz., singleplex i.e., detection of single
205 biomarkers either ER, PR or HER2 individually, then duplex with a combination of any two
206 out of three biomarkers and triplex analysis, which aimed to detect the expression status of all
207 the three biomarkers simultaneously in a single tissue specimen.

208 ***2.3.1 Singleplex analysis of tissue biomarkers by SERS-nanotags***

209 The first stage of clinical sample analysis was envisioned to detect a single biomarker either
210 ER/PR/HER2 in FFPE breast cancer tissue specimens. One of the major challenging factors in

211 the detection technique was the nonspecific binding of nanotags to the specimen, which may
212 lead to false positive results (**Figure S13**), thus reducing the specificity of the detection model.
213 To circumvent this stipulation, we have introduced an isotype antibody (IgG) conjugated SERS-
214 tag as a control with the respective singleplex nanotag (Wang et al., 2014) that provided a
215 ratiometric approach where the ratio of SERS intensity profile of ER / PR/ HER2 conjugated
216 SERS-nanotags and isotype control SERS-nanotags were measured. As shown in **Figure 1a**,
217 IHC confirmed ER positive tissue treated with AuNP@SDL@anti-ER SERS tag provided a
218 high-resolution Raman image and an average Raman intensity (ARI) corresponding to the
219 signature peak of SDL at 580 cm^{-1} demonstrating the sensitivity of ER nanotag. Similarly, from
220 different experiments, PR (**Figure 1b**) and HER2 (**Figure 1c**) positive tissues incubated with
221 SERS-nanotag (AuNP@MBA@anti-PR & AuNP@CV@anti-HER2) afforded distinct Raman
222 images and average spectrum with marker reporter peaks at 1084 (MBA) and $440\text{ (CV)}\text{ cm}^{-1}$
223 respectively. A ratio less than or equal to one is considered negative for that particular
224 biomarker where as a value greater than one is considered positive (**Table S1**). Therefore, the
225 formulated methodology by using RL-SERS-nanotags demonstrated a sensitive and specific
226 detection of the corresponding single biomarker in the FFPE breast cancer tissue specimens.
227



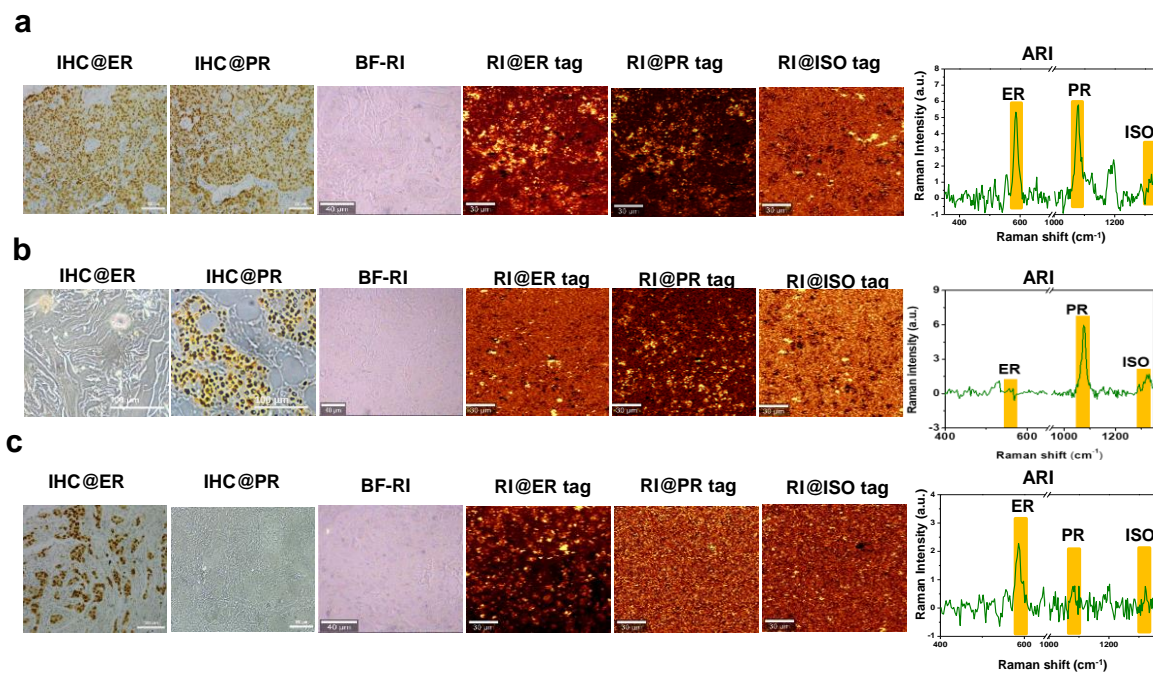
228

229 **Figure 1.** SERS singleplex analysis of a) ER⁺ b) PR⁺ and c) HER2⁺ tissue using
 230 AuNP@SDL@PEG@anti-ER, AuNP@MBA@PEG@anti-PR and AuNP@CV@PEG@anti-HER2
 231 nanotags along with AuNP@DTNB@PEG@anti-isotype tag. IHC-Immunohistochemistry
 232 confirmation for ER, PR and HER2 positivity of the specimens, BF-RI- Bright field images of the tissue
 233 area subjected for Raman image scanning, RI-Raman image corresponds to (a) 580 cm⁻¹ of
 234 AuNP@SDL@PEG@anti-ER, (b) corresponds to 1084 cm⁻¹ of AuNP@MBA@PEG@anti-PR and (c)
 235 corresponds to AuNP@CV@PEG@anti-HER2, RI@ISO tag corresponds the Raman images of
 236 AuNP@DTNB@PEG@anti-isotype., ARI-Average Raman intensity from the average scan spectrum of
 237 the ER⁺, PR⁺ and HER2⁺ tissue samples respectively.

238 2.3.2. Duplex analysis for tissue biomarkers by SERS-nanotags

239 Even though a few kits-based methods persisted, dual biomarker detection is a still challenging
 240 aspect to achieve through IHC. Using the current RL-SERS-tags, we have examined
 241 combinations of two biomarker analysis at a time, along with isotype control and investigated
 242 the differential expression status in a single tissue specimen. As shown in **Figure 2a**, luminal
 243 A tissue sample having ER⁺ PR⁺ expression was treated with SERS-tags conjugated to anti-ER
 244 (AuNP@SDL@anti-ER) and anti-PR (AuNP@MBA@anti-PR) antibodies. The average scan
 245 spectrum generated from the Raman image symbolized the presence of the signature peaks from
 246 SDL at 580 cm⁻¹ and MBA at 1084 cm⁻¹ with a ratiometric value >1 as compared to

247 AuNP@DTNB@Isotype confirming the specific recognition of ER and PR. Corresponding
 248 receptor negative samples viz., ER⁻PR⁺ (**Figure 2b**) and ER⁺PR⁻ tissues (**Figure 2c**) exhibited
 249 minimal SERS signals of SDL (580 cm⁻¹) and MBA (1084 cm⁻¹) respectively with a ratiometric
 250 value of <1. (**Table S2**). ER /HER2 and PR/HER duplexing were also experimented with to
 251 confirm the dual biomarker detection ability of the RL-SERS tags (**Figure S 14, Table S3**).

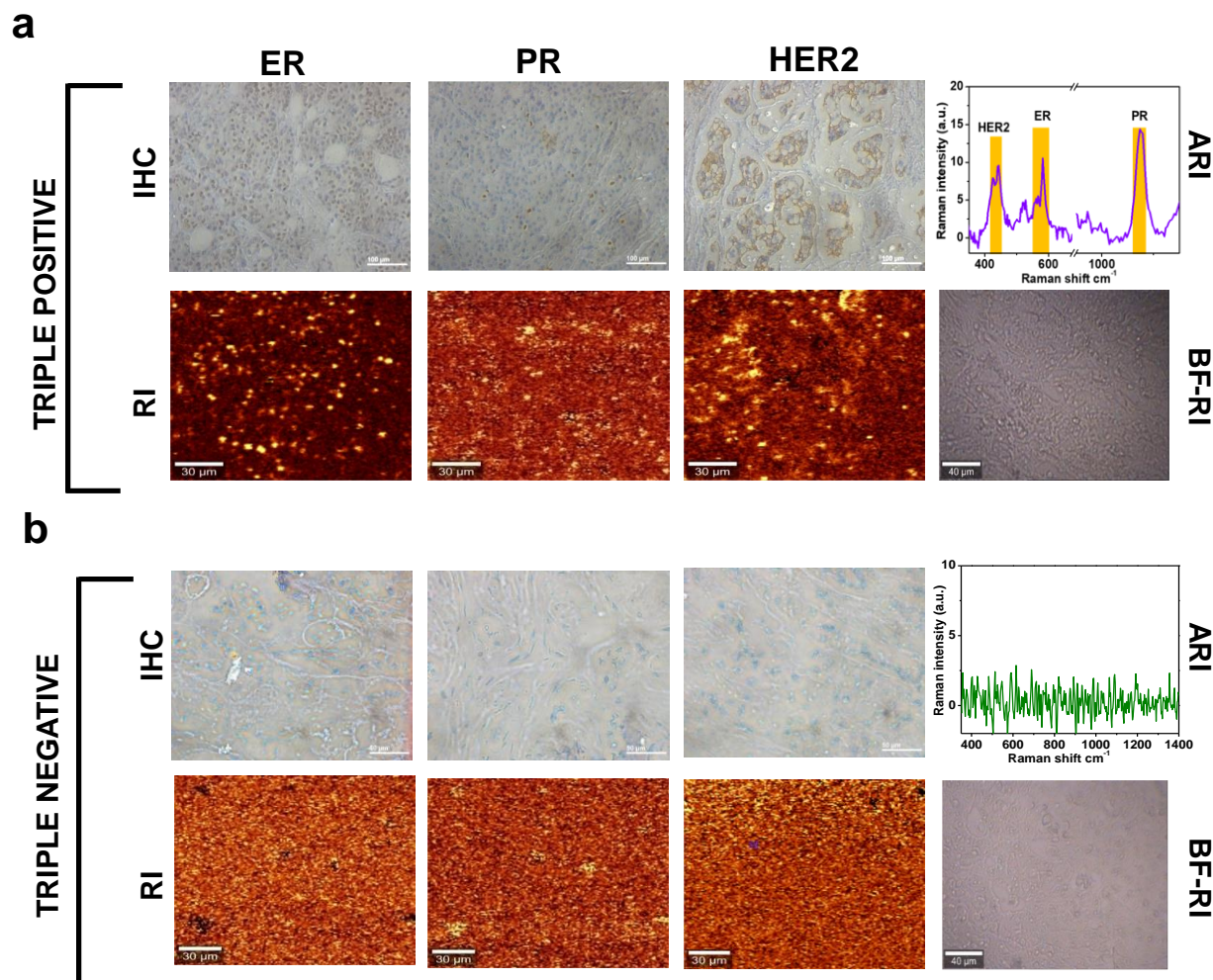


252
 253 **Figure 2.** SERS duplex analysis of a) of ER⁺ and PR⁺ tissue, b) ER⁻ and PR⁺ tissue and c) ER⁺ and PR⁻
 254 tissue samples using AuNP@SDL@PEG@anti-ER, AuNP@MBA@PEG@anti-PR and
 255 AuNP@CV@PEG@anti-HER2 nanotags along with AuNP@DTNB@PEG@anti-isotype tag. IHC-
 256 Immunohistochemistry confirmation for ER, PR and HER2 positivity of the specimens, BF-RI- Bright
 257 field images of the tissue area subjected for Raman image scanning, RI-Raman image corresponds to
 258 (a) 580 cm⁻¹ of AuNP@SDL@PEG@anti-ER, (b) corresponds to 1084 cm⁻¹ of
 259 AuNP@MBA@PEG@anti-PR and (c) corresponds to AuNP@CV@PEG@anti-HER2, RI@ISO tag
 260 corresponds the Raman images of AuNP@DTNB@PEG@anti-isotype, ARI-Average Raman intensity
 261 from the scan spectrum.

262

263 **2.3.3. Triplex analysis for tissue biomarkers in luminal B and basal tissue samples by RL-**
264 **SERS-nanotags**

265 In the set-up for triplex analysis, IHC confirmed luminal B (ER⁺PR⁺HER2⁺) tissue sample was
266 incubated with all the three SERS-nanotags i.e., AuNP@SDL@anti-ER, AuNP@MBA@anti-
267 PR and AuNP@CV@anti-HER2. SERS analysis revealed the recognition of ER, PR and HER2
268 biomarkers even in a single scan with its average spectrum having corresponding peaks of
269 SERS-nanotags at 580, 1084 and 440 cm⁻¹ with scanned images showing the receptor positive
270 and negative areas of the sample corroborating the detection of three biomarkers in a single
271 specimen (**Figure 3a**). Further, in another set, where IHC confirmed ER, PR and HER2
272 negative tissue (basal type) specimen was analysed with the SERS-tags, it showed negligible
273 Raman peaks for the three biomarkers (**Figure 3b**). A summarized data of tissue analysis is
274 shown in **Table S4**.



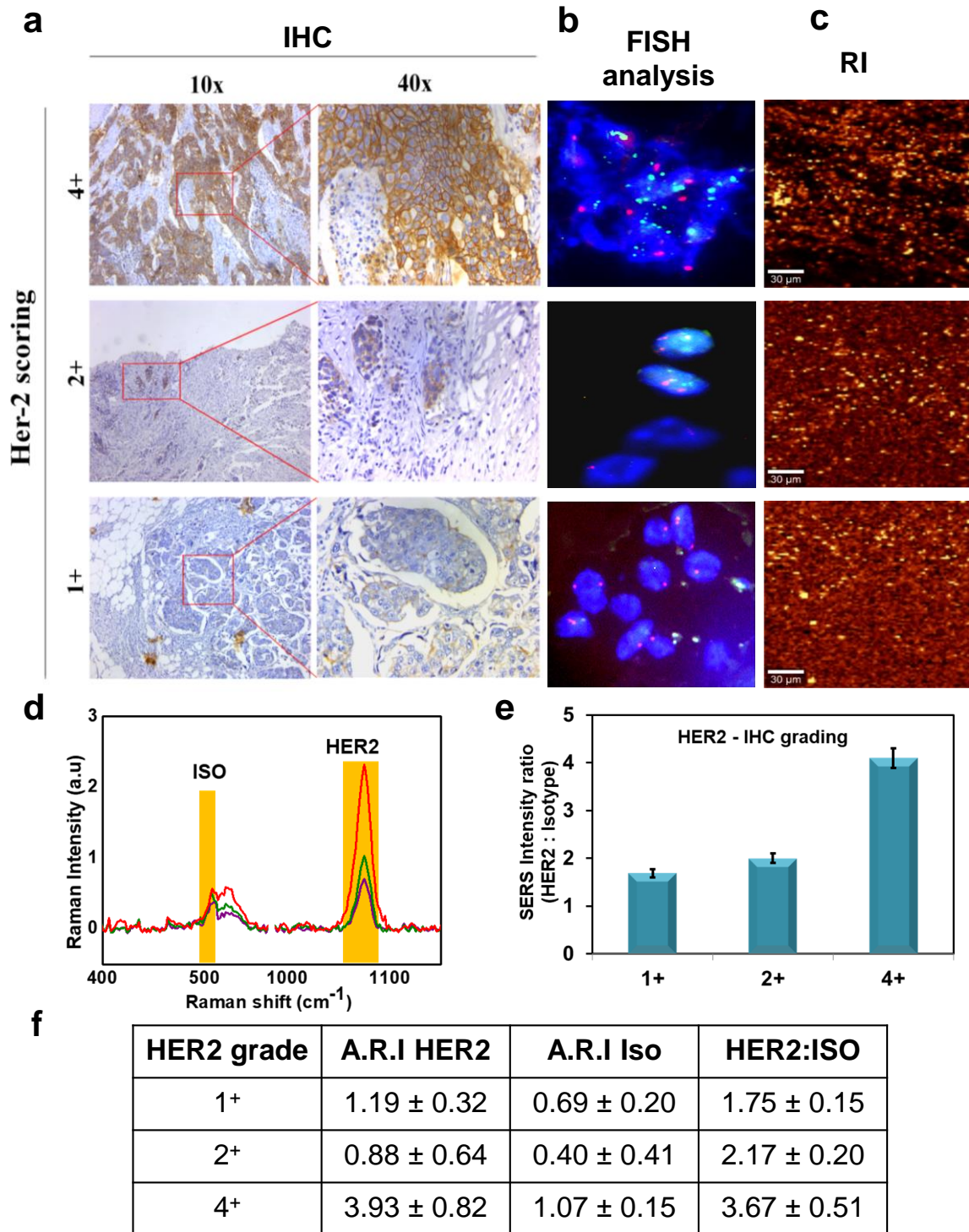
275

276 **Figure 3.** SERS analysis of a) Luminal B (ER⁺PR⁺HER2⁺) and b) Basal (ER-PR-HER2-) tissue using
 277 AuNP@SDL@anti-ER, AuNP@MBA@anti-PR and AuNP@CV@anti-HER2 nanotags. IHC-
 278 Immunohistochemistry confirmation for ER, PR and HER2 positivity of the specimens, BF-RI- Bright
 279 field images of the tissue area subjected for Raman image scanning, RI-Raman image corresponds to
 280 (a) 580 cm⁻¹ of AuNP@SDL@PEG@anti-ER, 1084 cm⁻¹ of AuNP@MBA@PEG@anti-PR and 440 cm⁻¹
 281 of AuNP@CV@PEG@anti-HER2, ARI-Average Raman intensity denotes the average scan spectrum
 282 of the duplex biomarkers in tissue samples respectively.

283 **2.4. HER-2 grading based on signature Raman label**

284 Unlike ER and PR, HER2 overexpression is considered for effective targeted therapy by the
 285 treatment of clinically approved trastuzumab. IHC grading of 3⁺ and more are judged to be
 286 HER2 positive, whereas 2⁺ / equivocal expression require further confirmation by FISH
 287 (Fluorescent in situ hybridization) analysis in which the number of HER2 gene copies per
 288 nucleus is assessed. This method is again a time-consuming and highly expensive technique in
 289 cytopathology. We introduced a ratiometric analysis of SERS-nanotag for measuring HER2

290 grading based on the signature Raman peak which precisely profiled the intensity ratio
291 between HER2-tag and isotype-control-tag. The Raman reporter DTTC was used for the isotype
292 antibody conjugated SERS-nanotag. As indicated in **figure 4**, IHC grades of 1⁺, 2⁺ and 4⁺ tissue
293 samples (**Figure 4a**) parallelly confirmed by FISH analysis (**Figure 4b**) were treated to Raman-
294 labeled SERS-tag (AuNP@MBA@anti-HER2) and isotype control SERS-tag
295 (AuNP@DTTC@Isotype) to assess the ratiometric analysis. **Figure 4c** revealed the Raman
296 scanned image, which indicated the gradation of HER2 expression. The Raman intensity profile
297 of the signature Raman label MBA (1084 cm⁻¹) and DTTC (505 cm⁻¹) designating HER2 -tag
298 and isotype-tag respectively is depicted in **Figure 4d**. The ratio of HER2-tag to isotype-tag
299 obtained from the average scan intensities is plotted in a bar diagram to get a mathematical
300 interpretation of the same (**Figure 4e**). Average SERS intensity from image scanning was found
301 to be higher for 4⁺ HER2 tissue with an intensity ratio of 3.67± 0.51 followed by 2⁺ HER2
302 (Ratio: 2.17± 0.2) and 1⁺ (Ratio: 1.75± 0.15) in harmony with the IHC staining pattern (**Figure**
303 **4 f**).



304

305 **Figure 4.** SERS analysis showing HER2 grading in HER2⁺ tissue using HER2 targeted
 306 AuNP@MBA@anti-HER2 and Isotype targeted AuNP@DTTC@anti-isotype nanotags. a) IHC
 307 analysis, b) FISH analysis (Orange fluorescence-for centromere (*CEP17*) of chromosome 17 as internal
 308 control, Green fluorescence - HER 2 gene), c) Raman Imaging (RI), d) Average Raman Intensity (ARI)
 309 and color representations, Purple (HER2¹⁺), Green (HER2²⁺), Red (HER2⁴⁺), e) representation of
 310 HER2 grading by bar diagram and f) table showing ratiometric signal values of HER2 versus isotype
 311 tags. Data, Average ± SD of three different analysis.

312 **2.5. Practical diagnostic applicability of RL-SERS-nanotags by large area SERS imaging**

313 The major bottleneck of our multiplexed SERS analysis in tissue samples was to screen the
314 entire area of the tissue specimen (usually of 5 to 10 mm² area) by Raman mapping since it
315 generally allows visibility up to 0.15 mm² to 0.2 mm² area only in minimal time. To accomplish
316 the total specimen analysis, large area Raman scanning technique was carried out with total
317 areas covering 0.5 as well as 5 mm². **Figure S15** demonstrates the large area scanning with 0.5
318 mm² area of the duplexing analysis, which was performed in various combinations like ER /PR,
319 PR / HER2 and ER/HER2 along with TNBC samples (**Figure S16**). The results illustrate the
320 large area scanning as a robust method to cover maximum tissue area to get more accuracy.
321 Owing to the excellent sensitivity of the SERS-nanotags, we have achieved a large area scan of
322 up to 5 mm², which provided a clear-cut idea about the prevalence of biomarkers in the sample.
323 This method was able to accurately detect different biomarkers in combination from the
324 scanning spectrum of gratifying resolution within 45 min scan duration (**Figure S17-S20**).
325 Considering the high throughput analysis of samples, still it is required to analyze many samples
326 at that stipulated time, which can be addressed by the advancements of current technologies in
327 future. A comparative analysis of conventional IHC and SERS techniques explaining the pros
328 and cons of both techniques is summarized in **Table 1**.

329

330

331

332

333

334

335 **Table 1:** Comparative pros and cons analysis of SERS vs IHC

Criteria	<i>Pros of SERS over IHC</i>	
	IHC	SERS
Multiplex detection of biomarkers	Difficult to attain due to the deficiency of standard methods	Easily possible
Sample preparation time	7-24 h	5-6 h
Secondary antibody and developing agents	Required	Not required
Analysis time	0.5 h/sample/one biomarker	1h/sample with multiple biomarker
Performance / Precision	Subjective due to the possibility of inter-observer error	Objective in nature and permits semiquantitative measurement
Criteria for biomarker grading	Based on percentage of stained cells and stain intensity	SERS mapping based on average spectral intensity
HER2 receptor grading	2 ⁺ /Equivocal samples required FISH confirmation	By ratiometric semi quantitative approach FISH confirmation can be justified
Criteria	<i>Cons of SERS over IHC</i>	
	IHC	SERS
Instrument cost	Inexpensive bright field histopathology microscope	Expensive Raman microscope is required
Clinical validation	Clinically validated technique	Clinical validation yet to be done
High throughput analysis	Automated systems are available	Advancement in the technique is required
Requirement of artificial intelligence (AI)	Not required	With the support of AI method, the technique can be improved for quantitative detection.

337 **3. Conclusion**

338 In summary, we have successfully introduced RL-SERS-nanotags based diagnostic platform
339 for the detection of clinically relevant breast cancer biomarkers in singleplex, duplex as well as
340 triplex fashion of IHC-confirmed breast cancer tissue subtypes. Optimized analysis mode of the
341 RL-SERS-nanotags along with untargeted isotype control SERS-nanotag rendered least non-
342 specific binding and ensured to minimize the false positive results. Moreover, HER2 grading
343 by ratiometric profiling of HER2 and isotype control tags eventually confirmed the 1⁺, 2⁺ and
344 4⁺ tissue samples were perfectly complementing with time-consuming IHC as well as expensive
345 FISH analysis. Finally, we have executed the whole area Raman mapping of a single specimen
346 with the multiplexing RL-SERS tags reflecting the capability of the newly emerged platform to
347 provide rapid results in less than an hour with minimal non-specific binding. The study thus
348 reveals a robust and highly sensitive diagnostic modality with futuristic potential for the
349 detection of tumors as well as tumor recurrence exhibiting differential biomarkers associated
350 with patient-to-patient heterogeneity. The inability of the system to perform high throughput
351 analysis in a fixed time may be improved by the introduction of advancements in
352 instrumentation in near future.

353 **4. Experimental Section**

354 Detailed methodology of nanoparticle synthesis, characterization, RR incorporation, antibody
355 conjugation, biocompatibility analysis, tissue processing methods and SERS analysis
356 parameters are provided in the supporting information.

357

358 **Supporting Information**

359 Supporting Information is available from the journal site.

360

361 **Acknowledgements**

362 Funding provided by CSIR Mission mode project, Nano-biosensor and Microfluidics for
363 Healthcare (HCP-0012) to perform this study is gratefully accredited by K.K.M., K.S. V.P.M.
364 thanks the CSIR mission mode project (HCP-0012), CSIR-FTT project, Customized Portable
365 Raman spectrophotometric device for multiplex detection of breast cancer biomarkers (MLP-
366 0039) and DHR Young Scientist program. VK acknowledges ICMR-SRF for research
367 fellowship, AcSIR Ph.D. student M.K.M thank UGC for research fellowship. D.S. and S.K.
368 thanks the CSIR mission mode project, Nano-biosensor and Microfluidics for Healthcare
369 (HCP-0012). A.L. acknowledges the CSIR mission mode project (HCP-0012) and DHR Young
370 scientist program (R.12014/22/2021-HR/E-office:8114716) , A.N.R thanks CSIR-SRF for
371 research fellowship. Authors are grateful to Dr Sudeep Gupta, Director, Advanced Centre for
372 Treatment, Research and Education in Cancer (ACTREC), Tata Memorial Centre, Mumbai,
373 India for the valuable suggestions and guidance. Author 1 and Author 2 contributed equally to
374 this work.

375 **Conflict of Interest**

376 The authors declare no conflict of interest.

377

378 **References**

- Bogdanovska-Todorovska, M., Kostadinova-Kunovska, S., Jovanovik, R., Krsteska, B.,
Kondov, G., Kondov, B., Petrushevska, G., 2018. Open Access Maced. J. Med. Sci. 6,
593–599.
- Cornejo, K.M., Kandil, D., Khan, A., Cosar, E.F., 2014. Arch. Pathol. Lab. Med. 138, 44–56.
- Costa, R.L.B., Czerniecki, B.J., 2020. npj Breast Cancer 6,10.
- Davis, R.M., Kiss, B., Trivedi, D.R., Metzner, T.J., Liao, J.C., Gambhir, S.S., 2018. ACS
Nano 12, 9669–9679.
- Dinish, U.S., Balasundaram, G., Chang, Y.T., Olivo, M., 2014. J. Biophotonics 7, 956–965.
- Dixon, A.R., Bathany, C., Tsuei, M., White, J., Barald, K.F., Takayama, S., 2015. Expert Rev.

- Mol. Diagn. 15, 1171–1186.
- Furrer, D., Sanschagrin, F., Jacob, S., Diorio, C., 2015. Am. J. Clin. Pathol. 144, 686–703.
- Haka, A.S., Shafer-Peltier, K.E., Fitzmaurice, M., Crowe, J., Dasari, R.R., Feld, M.S., 2005. Proc. Natl. Acad. Sci. U. S. A. 102, 12371–12376.
- Hernandez, S., Rojas, F., Laberiano, C., Lazcano, R., Wistuba, I., Parra, E.R., 2021. Front. Mol. Biosci. 8, 1–10.
- Joseph, M.M., Narayanan, N., Nair, J.B., Karunakaran, V., Ramya, A.N., Sujai, P.T., Saranya, G., Arya, J.S., Vijayan, V.M., Maiti, K.K., 2018. Biomaterials 181, 140–181.
- Lange, Carol A, D.Y., 2008. J. Mol. Endocrinol. 4, 151–162.
- Lee, S., Chon, H., Lee, J., Ko, J., Chung, B.H., Lim, D.W., Choo, J., 2014. Biosens. Bioelectron. 51, 238–243.
- Li, M., Kang, J.W., Sukumar, S., Dasari, R.R., Barman, I., 2015. Chem. Sci. 6, 3906–3914.
- Lin, C.Y., Yu, C.J., Lin, Y.H., Tseng, W.L., 2010. Anal. Chem. 82, 6830–6837.
- Lin, D., Hsieh, C.L., Hsu, K.C., Liao, P.H., Qiu, S., Gong, T., Yong, K.T., Feng, S., Kong, K.V., 2021. Nat. Commun. 12, 3430.
- Maiti, K.K., Dinish, U.S., Samanta, A., Vendrell, M., Soh, K.S., Park, S.J., Olivo, M., Chang, Y.T., 2012. Nano Today 7, 85–93.
- Narayanan, N., Karunakaran, V., Paul, W., Venugopal, K., Sujathan, K., Kumar Maiti, K., 2015. Biosens. Bioelectron. 70, 145–152.
- Nariman, B., Anne, F., Marie, H.J., Yubing, S., Byung, K., 2017. Nanotechnology 28, 455101.
- Njoki, P.N., Lim, I.I.S., Mott, D., Park, H.Y., Khan, B., Mishra, S., Sujakumar, R., Luo, J., Zhong, C.J., 2007. J. Phys. Chem. C 111, 14664–14669.
- Parise, C.A., Caggiano, V., 2014. J. Cancer Epidemiol. 2014; 469251.
- Ramya, A.N., Arya, J.S., Madhukrishnan, M., Shamjith, S., Vidyalekshmi, M.S., Maiti, K.K.,

2021. - *An Asian J.* 16, 409–422.
- Ramya, A.N., Samanta, A., Nisha, N., Chang, Y.T., Maiti, K.K., 2015. *Nanomedicine* 10, 561–571.
- Russo, J., Russo, I.H., 2006. *J. Steroid Biochem. Mol. Biol.* 102, 89–96.
- Schlücker, S., Salehi, M., Bergner, G., Schütz, M., Ströbel, P., Marx, A., Petersen, I., Dietzek, B., Popp, J., 2011. *Anal. Chem.* 83, 7081–7085.
- Shah, R., Rosso, K., David Nathanson, S., 2014. *World J. Clin. Oncol.* 5, 283–298.
- Sheng, W., Zhang, C., Mohiuddin, T.M., Al-rawe, M., Zeppernick, F., Falcone, F.H., Meinhold-heerlein, I., Hussain, A.F., 2023. *Int. J. Mol. Sci.* 24, 3086. Sun, J., Li, W., Zhu, X., Jiao, S., Chang, Y., Wang, S., Dai, S., Xu, R., Dou, M., Li, Q., Li, J., 2021. *J. Agric. Food Chem.* 69, 11494–11501.
- Tan, W.C.C., Nerurkar, S.N., Cai, H.Y., Ng, H.H.M., Wu, D., Wee, Y.T.F., Lim, J.C.T., Yeong, J., Lim, T.K.H., 2020. *Cancer Commun.* 40, 135–153.
- Wang, Y., Kang, S., Doerksen, J.D., Glaser, A.K., Liu, J.T.C., 2016. *IEEE J. Sel. Top. Quantum Electron.* 22, 6802911.
- Wang, Y., Reder, N.P., Kang, S., Glaser, A.K., Yang, Q., Wall, M.A., Javid, S.H., Dintzis, S.M., Liu, J.T.C., 2017. *Cancer Res.* 77, 4506–4516.
- Wang, Y. “Winston,” Khan, A., Som, M., Wang, D., Chen, Y., Leigh, S.Y., Meza, D., McVeigh, P.Z., Wilson, B.C., Liu, J.T.C., 2014. *Technology* 02, 118–132.
- Wang, Y., Yan, B., Chen, L., 2013. *Chem. Rev.* 113, 1391–1428.
- Wang, Y.W., Doerksen, J.D., Kang, S., Walsh, D., Yang, Q., Hong, D., Liu, J.T.C., 2016. *Small* 12, 5612–5621.
- Wesoła, M., Jeleń, M., 2015. *Adv. Clin. Exp. Med.* 24, 899–904.
- Zavaleta, C.L., Garai, E., Liu, J.T.C., Sensarn, S., Mandella, M.J., Van De Sompel, D., Friedland, S., Van Dam, J., Contag, C.H., Gambhira, S.S., 2013. *Proc. Natl. Acad. Sci. U. S. A.* 110, E2288-97.

TOC

Raman spectroscopy driven histopathologic approach have been evolved for the clinical diagnostics utilizing targeted Raman-label-SERS (RL-SERS)-nanotags which ensures a rapid, sensitive and accurate multiplexed detection of clinically relevant breast cancer biomarkers, ER, PR and HER2 in single tissue specimen by the marked signature Raman fingerprint resembling the corresponding biomarker.

A Clinically Feasible Diagnostic Spectro-Histology Built on SERS-Nanotags for Multiplex Detection and Grading of Breast Cancer Biomarkers

ToC figure

